Distributed Power Allocation Based on LQG Regulator With Adaptive Weight and Switching Scheme for Cognitive Radio Networks

SHUYING ZHANG AND XIAOHUI ZHAO, (Member, IEEE)

College of Communication Engineering, Jilin University, Changchun 130012, China

Corresponding author: Xiaohui Zhao (xhzhao@jlu.edu.cn)

ABSTRACT We present a distributed power allocation algorithm for a cognitive radio network (CRN), where the underlying secondary users (SUs) share the same licensed spectrum with the primary users (PUs). Based on the target signal-to-interference-plus-noise ratio (target-SINR) tracking power control (TPC) algorithm in a conventional network, the power allocation problem is modeled as a state-space model with exogenous input that includes varying channel state information (CSI) and some parameter measurement errors. This power allocation algorithm is actually a state feedback controller from the linear quadratic Gaussian (LQG) solution, which is used to guarantee the SINR requirement of the SUs and keep the interference temperature (IT) constraint of all PUs under a given threshold. Considering the quality of service (QoS) of the SU, an adaptive control weight and a switching safety margin of the IT threshold are introduced in this algorithm to achieve better performance. Analysis and simulation results show the effectiveness and advantages of the proposed power allocation scheme, designed based on control theory, compared with those of other traditional algorithms designed based on optimization.

INDEX TERMS Cognitive radio, power allocation, state-space description, closed-loop control, linear quadratic Gaussian regulator.

I. INTRODUCTION

Power allocation in a cognitive radio network (CRN) is an important research topic in the area of wireless communication systems for high spectrum efficiency [1]. It is well known that the secondary users (SUs) can use spectral resources licensed to the primary users (PUs) without interrupting the primary communication in a CRN. However, this reuse of the spectrum inevitably leads to mutual interference among users. Therefore, a reasonable power allocation scheme should be developed according to the communication requirements and environment to ensure the coexistence of PUs and SUs in CRNs.

The power allocation problem for a CRN is easily solved by centralized algorithms, which need all information about the current network [2], [3]. These algorithms are often based on the assumption that all known information does not have measurement errors so that they can perform better to meet the quality of service (QoS) for all users. However, this assumption is more or less impractical when considering an actual communication system. First, it requires much overhead to send the information, taking up much bandwidth. Additionally, more information and its measurement will result in more time delays and errors. To reduce the use of global information for centralized power allocation, some interesting distributed power allocation methods that use local information, which are more reliable and practical than those of the centralized methods, have been proposed in [4]–[6].

Categorizing the existing studies on the distributed power allocation algorithms for CRNs, we find that the majority use the optimization theory to maximize or minimize one or more target functions parameterized by the communication performance subject to some constraints and a protection mechanism for PUs, for example, the interference temperature (IT) constraint, the outage probability constraint of the PU and so on [7]–[9]. This approach needs all current channel state information (CSI) to calculate an optimal transmit power sequence, which makes it very sensitive to

different disturbances, uncertainties and time delays, which are inevitable in CRNs. There are some methods for solving this problem. Specifically, to address the influence of channel uncertainty, methods based on the robust optimization theories, such as the Bayesian approach and the worst-case approach, have been used [10], [11]. However, these methods require some prior knowledge, which is difficult to obtain, and they are conservative because of the formulation of all disturbances, errors and time delays as a worst or statistical uncertainty. Moreover, the traditional power allocation algorithms are not dynamic in the sense of a dynamic description of a CRN. The optimization solution is determined via static modeling of the problem in one time slot. And it is only an approximation of the problem but not applicable. The technological framework still remains used on the research of this issue though it has been extended in various ways, such as introduction of new model, complexity reduction, diversity improvement, new objective optimization, application consideration and so on [12]–[15].

When we consider a time-varying channel, stochastic uncertainty, different estimation errors, the time delay, random changing of users and the different QoS requirements for a CRN, power allocation becomes a dynamic process in which the transmit power of each active SU should be dynamically adjusted based on the instantaneous objective function, all available information and the varying environment.

Control theories normally or basically provide us with a useful tool for designing a closed-loop controller when considering the dynamic property of a target system described either by a state-space description, an input-output description or a differential equation. Those methods based on these theories have been proven to be effective in almost every domain of industry and even in social systems with very precise control. They have already been used in some conventional wireless networks to provide a dynamic way to address the power control problem [16]–[20], most of which are based on the target signal-to-interference-plus-noise ratio (target-SINR) tracking power control (TPC) algorithm, also called standard power control. These studies indicate that we can design a feedback controller to realize power allocation for wireless networks with robustness against measurement errors, channel uncertainty, and time delays. Since the power allocation problem does not need high-precision control and requires only that certain interference constraints be kept under some requirements with enough high object, we can use control theory to effectively solve this problem in a dynamic way that is more realistic and practical compared with those approaches based on convex optimization or game theory.

Recently, some studies based on control theory have been proposed to analyze and solve some real problems of power allocation in CRNs. The authors in [21] analyze the stability-related problem of power control in multiple coexisting wireless networks based on small-gain theorem. In [7] and [22], the authors present the analysis of the transient behavior of a CRN based on the modeling of the power allocation problem

as a projected dynamic system (PDS) by variational inequality. These fundamental works provide us with an interesting research direction with the possibility and feasibility of using control theory to solve the power allocation in a CRN. However, they do not give us a feedback controller in the sense of closed-loop control for the problem. In [23], the authors also propose a robust power allocation scheme based on control theory for orthogonal frequency division multiplexing (OFDM)-based CRNs, where a closed-loop controller is designed for the PDS proposed in [7]. However, the control model is for a particular CRN and its mathematical derivation is very complicated so that the controller design is difficult.

According to our study, we find that, comparing with the power allocation of traditional non-cognitive networks, the IT constraint in a CRN is the main obstacle for using the control theory to solve the problem of CRNs since we have to obtain the control target to design a realized controller from a physically measured signal. The authors in [24] introduce PID control and model predictive control (MPC) to solve the power allocation problem, where the actual transmit power is determined by comparing the derived transmit power with a constraint condition to avoid interference with the primary networks; however, some parametric uncertainties are not considered. In [25], the authors propose an energy-saving adaptive transmit power control scheme based on bit error rate (BER) feedback for a cognitive personal area network (CPAN) in the multiband orthogonal frequency division multiplexing (MB-OFDM) ultra-wideband (UWB) system. In this scheme, each CPAN device controls its transmit power using a nonlinear approximation of the power-time curve to make the total power in an MB-OFDM band and the BER lower than the corresponding acceptable threshold. However, they consider only the total power constraint in an MB-OFDM band and not the interference from a SU to PUs, which may result in serious disturbance of the primary links. In general, it is not direct and easy to manipulate control theory to design a power controller for a CR system without suitably modeling the dynamics of this CRN with the IT constraint [7], which is one of the most important and available control requirements.

In this paper, based on the TPC algorithm, we remodel the problem of power allocation in a CRN by following dynamic control theory, where the IT constraint and QoS requirement of SUs are formulated as state variables and a cost function. Then, we design the corresponding state feedback controller to minimize the cost function. Furthermore, to improve the QoS of this CRN, we modify the proposed power control scheme by introducing an adaptive control weight and a switching safety margin of the IT threshold.

The major contributions of this paper are as follows:
- Based on the description of the channel gain fluctuation as a first-order Markov model, we formulate the dynamics of the power allocation problem in a CRN as a linear state-space model with exogenous input by its decibel scale, which is the basis of the closed-loop

controller design of the CRN, to solve this problem via the control method. This dynamic model is simple and general with respect to the power allocation problem of a CRN and provides a greater possibility of using different control theories.

- Considering varying channel gains and measurement errors of the parameters, we propose a distributed power allocation algorithm for the given CRN, named the linear quadratic Gaussian (LQG) regulator, to optimize the control performance index, including the IT constraint and QoS of the SU, to obtain a feasible target-SINR and a reasonable transmit power.

- According to the given basic LQG regulator, we also propose an improved controller with an adaptive control weight and a switching safety margin of the IT threshold to address the varying environment. We present the analysis of the proposed power allocation algorithm, which involves a performance comparison, in terms of the outage ratio of the PU and the SU and the total data transmission rate, with other typical power allocation algorithms.

The layout of the paper is as follows. Section II introduces the network model in a state-space representation. The formulation of the power allocation problem based on the state-space model and the power controller design are given in Section III. The improved version with an adaptive control weight and the switching safety margin of the IT threshold are given in Section IV. Section V presents the analysis of the proposed power allocation algorithm. The simulation results are provided in Section VI, and conclusion is drawn in Section VII.

II. CRN MODEL

We consider the CRN that is schematically presented in Fig. 1. In this given model, there is a primary cellular network coexisting with a secondary arbitrary network. The primary network is composed of one PU base station (PU-BS) and L PU receivers (PU-RXs) with index l, $l \in \mathcal{L}$ and $\mathcal{L} = \{1, \cdots, L\}$. The secondary network has M SU transmitter (SU-TX) and SU receiver (SU-RX) pairs with index i, $i \in \mathcal{M}$ and $\mathcal{M} = \{1, \cdots, M\}$. Since the practical power control algorithms are usually implemented in discrete-time, we directly present the discrete-time version of our power control algorithm. In this CRN, the power adjustment time for a packet is divided into 32 slots, and each slot period T_s, in which power control, including signal measurement, feedback and the corresponding information update, is conducted, is appropriately chosen. We mainly study the power control for SUs at the downlink time of the PU, namely, in the channels from the BS to the mobile terminals. However, the following obtained results can also be used in the uplink case, i.e., in the channels from the mobile terminals to the BS.

In the CRN, the communication of the PU is protected by the IT constraint such that the interference from SUs to the lth PU must be below a corresponding threshold, which is
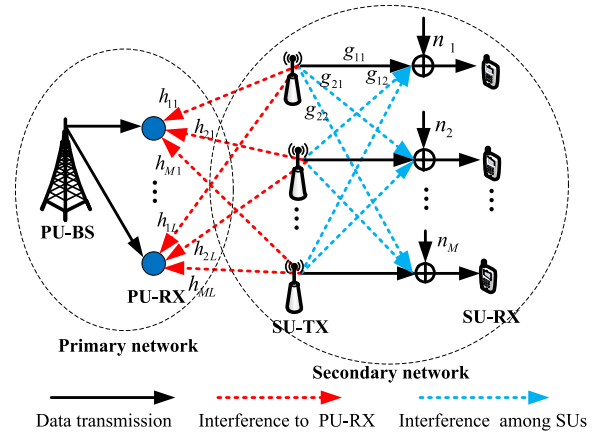

FIGURE 1. CRN model.

described as

$$I^l(k) = \sum_{i \in \mathcal{M}} h_i^l(k) p_i(k) \leq I_{th}^l, l \in \mathcal{L} \qquad (1)$$

where $h_i^l(k)$ is the interference gain at the time slot k between the ith SU-TX and the lth PU-RX, $p_i(k)$ is the transmit power of the ith SU and I_{th}^l is the predefined IT threshold of the lth PU, its value would be a maximum amount of tolerable interference for a given frequency band in a particular location and can be determined according to a given IT model like [26]. Note that the channel gain represents the channel power gain unless otherwise noted in this paper. Since SUs are coupled by (1), power control cannot be completed by using only local information. Moreover, it is impractical or even impossible for each SU to know the interference at PU-RX caused by all SUs, including itself. Thus, we replace this interference constraint with the sum of transmit power of all SUs, with an individual constraint on each SU to address (1) according to [27], where we call it average IT constraint. And the QoS requirement for the lth PU can be easily guaranteed as long as the following average IT constraint

$$I_i^l(k) = h_i^l(k) p_i(k) \leq I_{avg}^l \qquad (2)$$

is held, where $I_{avg}^l = I_{th}^l / M$ is the average IT threshold. Using the new constraint will introduce somewhat conservativeness, but it greatly simplifies the designing distributed power control algorithm under the premise of ensuring data transmission of SU without communication interruption of PU in the CRN.

In power control algorithm design, it is difficult to address the multiplication relation in (2). To simplify the subsequent control model, we use the decibel scale $\bar{x} = 10 \lg(x)$ to represent a variable. Substituting the variables of (2) with the decibel values, we can obtain the following linear equation:

$$\bar{I}_i^l(k) = \bar{h}_i^l(k) + \bar{p}_i(k) \leq \bar{I}_{avg}^l \qquad (3)$$

For the secondary network, we regard the SINR of each SU as a performance metric for power control, as the measured SINR at the receiver's antenna is a parameter directly related

to the carrier power, which can be controlled by transmit power adjustment. In the CRN, the instantaneous SINR of the ith SU is described by

$$\gamma_i(k) = \frac{g_{ij}(k)p_i(k)}{\sum_{j \neq i} g_{ij}(k)p_j(k) + I_i^{ps}(k) + n_i^2} \quad (4)$$

where $g_{ij}(k)$ is the channel gain from the jth SU-TX to the ith SU-RX at the time slot k and $\sum_{j \neq i} g_{ij}(k)p_j(k)$ and $I_i^{ps}(k)$ are the interferences at the ith SU-RX from other SUs and all PUs, respectively. n_i^2 is the background noise power. We define $I_{-i}^{ss}(k) = \sum_{j \neq i} g_{ij}(k)p_j(k) + N_i^2$ to represent the interference plus noise at the ith SU-RX, where $N_i^2 = I_i^{ps}(k) + n_i^2$ is regarded as the generalized background noise power, including the interference from the PUs to SU i, the value of which is assumed to be measurable and invariable in a packet transmission. In addition, each SU can utilize a quiet period as in IEEE 802.22 WRANs to measure the interference from primary transmissions since there is only a primary transmission in this period [28]. Alternatively, we use $\mu_i(k) = \frac{g_{ii}(k)}{I_{-i}^{ss}(k)}$ to represent the effective channel gain of the ith SU; then, (4) becomes $\gamma_i(k) = \mu_i(k)p_i(k)$. After carrying out the same transformation from (2) to (3), the SINR of the ith SU at the decibel scale is

$$\bar{\gamma}_i(k) = \bar{\mu}_i(k) + \bar{p}_i(k) \quad (5)$$

Our purpose is to design a distributed power controller by using only local information to allocate power for each SU. To realize this goal, the dynamics modeling of this CRN must be carried out.

In wireless networks, varying channel gain is a combination of slow shadow fading and fast multipath fading on top of path loss. In this paper, we assume that the period of update power T_s is more than the coherence time of the channel, the maximum time difference range in which the channel remains the same fading properties. Therefore the multipath influence will be negated in this channel model. We consider the case where the lognormal distribution shadow fading and the relative distance between two users does not change in 32 slots, which means that the change in the channel gain depends only on the shadow fading during the power adjustment process for a packet.

According to [16], the spatial correlation of the channel gain at the decibel scale can be described as a simple first-order Markov random model when the shadow fading is dominant. Taking the ith SU, the first-order Markov random model of its channel gain can be written as

$$\bar{g}_{ii}(k) = \bar{g}_{ii}^0 + \Delta \bar{g}_{ii}(k) \quad (6)$$
$$\Delta \bar{g}_{ii}(k) = a \Delta \bar{g}_{ii}(k-1) + \bar{\omega}_{g_{ii}}(k-1) \quad (7)$$

where $\bar{g}_{ii}^0$ is a constant bias, $\bar{\omega}_{g_{ii}}$ is the zero-mean white Gaussian random sequence, $a = \exp\left(-\frac{vT_s}{X_s}\right)$, with moving velocity v of the user and varying distance vT_s during a time slot, and X_s is the decorrelation distance.

From (6) and (7), we can obtain

$$\bar{g}_{ii}(k) = a \bar{g}_{ii}(k-1) + (1-a)\bar{g}_{ii}^0 + \bar{\omega}_{g_{ii}}(k-1) \quad (8)$$

When the SU is assumed to not move, i.e., $v = 0$, resulting in $a = 1$ in (8), we have

$$\bar{g}_{ii}(k) = \bar{g}_{ii}(k-1) + \bar{\omega}_{g_{ii}}(k-1) \quad (9)$$

Through the same modeling process with channel gain of SU, we formulate the dynamics of the interference plus noise $I_{-i}^{ss}(k)$ of the ith SU and the channel gain of PU as follows

$$\bar{I}_{-i}^{ss}(k) = \bar{I}_{-i}^{ss}(k-1) + \bar{\omega}_{I_{-i}^{ss}}(k-1) \quad (10)$$
$$\bar{h}_i^l(k) = \bar{h}_i^l(k-1) + \bar{\omega}_{h_i}^l(k-1) \quad (11)$$

where $\bar{\omega}_{I_{-i}^{ss}}$ and $\bar{\omega}_{h_i}^l$ are also the zero-mean white Gaussian random sequences. Although (10) cannot precisely describe the dynamics of $I_{-i}^{ss}(k)$ at all times, it is still reasonable when the shadow fading is dominant in the channel gain [29]. Furthermore, the dynamics of the effective channel gain of the ith SU at the decibel scale can be determined by

$$\bar{\mu}_i(k+1) = \bar{\mu}_i(k) + \bar{\omega}_{\mu_i}(k) \quad (12)$$

where $\bar{\omega}_{\mu_i}(k) = \bar{\omega}_{g_{ii}}(k) - \bar{\omega}_{I_{-i}^{ss}}(k)$ is also the zero-mean white Gaussian random sequence.

In previous distributed power control schemes, an assumption that the channel remains constant despite the interference plus noise of the ith SU during a packet transmission is often required [24]. In fact, for practical communication, this assumption is strong and ideal when the wireless channel differs for different time slots, even when the mobile terminal does not move. At the same time, the interference from another user to the SU changes as the transmit power of other users changes. Thus, the use of random sequences $\bar{\omega}_{\mu_i}$ and $\bar{\omega}_{h_i}^l$ to model the dynamics of the channel gain for a wireless communication environment is closer to reality.

III. PROBLEM FORMULATION AND STATIC CONTROLLER DESIGN

In this section, we build a state-space model to formulate the power allocation problem of the CRN. Under this model, we propose a distributed power control scheme based on the LQG regulator.

In a non-cognitive network, the conventional methods used to control the transmit power are normally designed as target tracking algorithms for the given QoS benchmark, which is often given in a fixed or time-varying SINR form. Generally, the power control process in a code division multiple access (CDMA) network is divided into two parallel parts: inner loop and outer loop. In the inner loop, the user adopts a TPC algorithm [30] to make the received SINR track the given target-SINR provided by the outer loop. In the outer loop, the procedure for updating the target-SINR usually depends on the communication requirement of users and the current network status. In this study, we also adopt this

flexible QoS benchmark to control the transmit power for each SU in the CRN described in Section II.

Note that the applicability of a dynamic control method based on the flexible QoS service depends on the feasibility of the fast target QoS tracking [16], [19]. In traditional cellular communication, varying target-SINR is provided by the outer control loop according to the network requirements, such as the transmission rate or BER. Moreover, the update frequency of the target-SINR in the outer loop is lower than that of the transmit power. For the current networks or even 5G networks, the update period for the target-SINR in one time slot is also supported by the rapid development of hardware technology, which allows flexible target-SINR tracking in communications [19].

We describe the process of power control using a cascade block diagram, as shown in Fig. 2, where the SU-RX uses an outer loop controller to update the target-SINR based on the information from the environment, including the instantaneous SINR and the interference affecting the PUs, and the update period of the target-SINR is one time slot, as mentioned above.
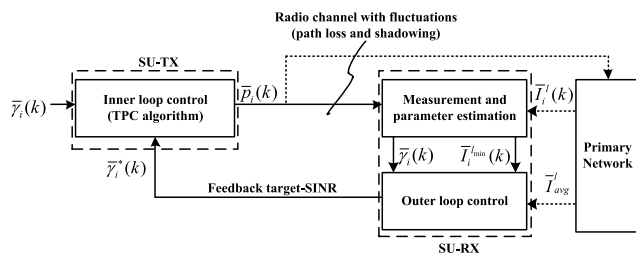

FIGURE 2. Block diagram of the ith SU transceiver pair.

The power control law of the TPC algorithm for the system in Fig. 2 is

$$\bar{p}_i(k+1) = \bar{p}_i(k) + \alpha_i \left[\bar{\gamma}_i^*(k) - \bar{\gamma}_i(k) \right] \qquad (13)$$

where $0 < \alpha_i < 1$ is the control gain of TPC algorithm, which varies from one link to another to provide the "smoothing" change of transmit power from one time slot to the next when $\bar{p}_i(k+1)$ is not larger than $\bar{p}_i^{max}$. The initial power $\bar{p}_i(0)$ is also assumed to be different in different links. In (13), the variable $\bar{\gamma}_i^*(k)$ is the decibel form of the time-varying target-SINR $\gamma_i^*(k)$. In our CRN, the normal communication of SUs needs to be guaranteed, and the interference affecting the PUs should be kept below a given threshold. To satisfy the communication requirements for both the SUs and PUs, we introduce an auxiliary control $u_i(k)$ for the target-SINR to realize the tracking of $\bar{\gamma}_i^*(k)$ by the instantaneous SINR $\bar{\gamma}_i(k)$. The feasible $\bar{\gamma}_i^*(k)$ ensures that the interference power with respect to the PU is below the IT threshold at a given time; the communication requirement of each SU can be satisfied if $\bar{\gamma}_i(k)$ reaches $\bar{\gamma}_i^*(k)$. The iterative updating of $\bar{\gamma}_i^*(k)$ is expressed as

$$\bar{\gamma}_i^*(k+1) = \bar{\gamma}_i^*(k) + u_i(k) \qquad (14)$$

We know that the obtained $\bar{\gamma}_i^*(k)$ is available in a practical environment only when the current channel state is good enough to support communication by the active SU and the allocated power for each SU lies within the allowable range. When too many active SUs generate an excessive amount of traffic, the called admission control should be used to guarantee satisfactory services for the admitted SUs. The focus of this research is power allocation rather than admission control of the CRN; thus, we assume that the number of current SUs is reasonable such that all services can be ensured. In addition, we do not consider the maximum power constraint of SU when we design our power controller because the traffic of the SU can be assumed to drop when the allocated power is outside its own range or when the power can be directly set as $\bar{p}_i^{max}$.

Substituting (12), (13) and (14) into (5), we can obtain a new representation for $\bar{\gamma}_i(k)$:

$$\bar{\gamma}_i(k+1) = (1 - \alpha_i)\,\bar{\gamma}_i(k) + \alpha_i \bar{\gamma}_i^*(k) + \bar{\omega}_{\mu_i}(k) \qquad (15)$$

To establish the relation between the target-SINR and the IT constraint, we substitute (11) and (13) into (3) to obtain the difference equation of the interference affecting the PU, i.e.,

$$\bar{I}_i^l(k+1) = \bar{I}_i^l(k) + \alpha_i \left[\bar{\gamma}_i^*(k) - \bar{\gamma}_i(k) \right] + \bar{\omega}_{h_i}^l(k) \qquad (16)$$

Our work aims to select a power control sequence $\{p_i(k)\}$ such that the actual SINR of the SU must approach as closely as possible the target one defined by (14) subject to the given IT constraint. In the CRN, the existence of the IT constraint makes the power control different compared with that in a non-cognitive network. Hence, control theory must be used for power allocation on the basis of the dynamic description of the CRN with the IT constraint via a feasible state-space model. In particular, we convert this constraint into a performance index and minimize it using a feasible controller.

We introduce two state variables $\bar{\varepsilon}_i^{ss}(k)$ and $\bar{\varepsilon}_i^l(k)$, defined as the error between the target-SINR and its actual value and that between the IT threshold and its actual value, respectively, as follows

$$\bar{\varepsilon}_i^{ss}(k) = \bar{\gamma}_i^*(k) - \bar{\gamma}_i(k) \qquad (17)$$
$$\bar{\varepsilon}_i^l(k) = \bar{I}_{avg}^l - \bar{I}_i^l(k) \qquad (18)$$

Their difference equations are

$$\bar{\varepsilon}_i^{ss}(k+1) = (1 - \alpha_i)\,\bar{\varepsilon}_i^{ss}(k) + u_i(k) - \bar{\omega}_{\mu_i}(k) \qquad (19)$$
$$\bar{\varepsilon}_i^l(k+1) = -\alpha_i \bar{\varepsilon}_i^{ss}(k) + \bar{\varepsilon}_i^l(k) - \bar{\omega}_{h_i}^l(k) \qquad (20)$$

Then, we define an element state vector $\mathbf{x}_i(k) = \left[\bar{\varepsilon}_i^{ss}(k),\ \bar{\varepsilon}_i^1(k), \cdots, \bar{\varepsilon}_i^L(k) \right]^T$, with $L + 1$ dimensions, for the SU link i. Combining (19) with (20), we establish the general state-space model for this link as

$$\mathbf{x}_i(k+1) = \mathbf{A}_i \mathbf{x}_i(k) + \mathbf{B}_i^1 \mathbf{w}_i(k) + \mathbf{B}_i^2 u_i(k) \qquad (21)$$

where the coefficient matrices are as follows:

$$\mathbf{A}_i = \begin{bmatrix} 1-\alpha_i & 0 & 0 & \cdots & 0 \\ -\alpha_i & 1 & 0 & \cdots & 0 \\ -\alpha_i & 0 & 1 & \cdots & 0 \\ \vdots & \vdots & \vdots & \ddots & \vdots \\ -\alpha_i & 0 & 0 & \cdots & 1 \end{bmatrix}_{(L+1)\times(L+1)} \tag{22}$$

$$\mathbf{B}_i^1 = \begin{bmatrix} -1 & \cdots & 0 \\ \vdots & \ddots & \vdots \\ 0 & \cdots & -1 \end{bmatrix}_{(L+1)\times(L+1)} \tag{23}$$

$$\mathbf{B}_i^2 = \begin{bmatrix} 1 & 0 & \cdots & 0 \end{bmatrix}_{(L+1)\times 1}^T \tag{24}$$

The fluctuation about the corresponding channel gain $\mathbf{w}_i(k)$ can be considered as an exogenous disturbance in this state-space model and defined as a vector

$$\mathbf{w}_i(k) = \begin{bmatrix} \bar{\omega}_{\mu_i}(k), \bar{\omega}_{h_i}^1(k), \cdots, \bar{\omega}_{h_i}^L(k) \end{bmatrix}^T \tag{25}$$

whose property will be discussed later.

Regarding the control of (21), we must verify its controllability, which is necessary for a control problem described by the state-space model. We calculate the controllability matrix as (26), as shown at the bottom of this page. Clearly, the rank of this matrix is only 2 instead of $L + 1$, which means that this state model is not controllable. The reason is that there is only one working interference entry, which must belong to the most vulnerable PU. Therefore, in the process of power control, we need to consider only this interference entry of the corresponding link from the SU to the PU at every instance of time so that the interference of other links can be satisfactorily restricted. From this discussion, we define $l_{\min}$ as the index of the PU whose transmission is the most easily disturbed. The way to obtain $l_{\min}$ is to select the index with the minimal distance between the IT threshold and its actual interference, which is given as

$$l_{\min} = \arg \min_l \left\{ \bar{I}_{avg}^l - \bar{I}_i^l(k) \right\} \tag{27}$$

Considering only the error between the IT threshold and the actual value of interfenence in the primary link $l_{\min}$, we modify (21) as

$$\tilde{\mathbf{x}}_i(k+1) = \tilde{\mathbf{A}}_i \tilde{\mathbf{x}}_i(k) + \tilde{\mathbf{B}}_i^1 \tilde{\mathbf{w}}_i(k) + \tilde{\mathbf{B}}_i^2 u_i(k) \tag{28}$$

where $\tilde{\mathbf{x}}_i(k) = \begin{bmatrix} \bar{\varepsilon}_i^{ss}(k), \varepsilon_i^{l\min}(k) \end{bmatrix}^T$ is the state vector, $\tilde{\mathbf{A}}_i = \begin{bmatrix} 1-\alpha_i & -\alpha_i \\ -\alpha_i & 0 \end{bmatrix}$, $\tilde{\mathbf{B}}_i^1 = \begin{bmatrix} -1 & 0 \\ 0 & -1 \end{bmatrix}$ and $\tilde{\mathbf{B}}_i^2 = \begin{bmatrix} 1 \\ 0 \end{bmatrix}$ are the

coefficient matrices, and $\tilde{\mathbf{w}}_i(k) = \begin{bmatrix} \bar{\omega}_{\mu_i}(k), \bar{\omega}_{h_i}^{l\min}(k) \end{bmatrix}^T$ is the coefficient exogenous disturbance vector. Since the controllability matrix is now full rank, the state model of (28) is controllable.

To achieve the power allocation objective, we design a controller that makes $\left| \bar{I}_{avg}^{l\min} - \bar{I}_i^{l\min}(k) \right|$ and $\left| \bar{\gamma}_i^*(k) - \bar{\gamma}_i(k) \right|$ as small as possible during a period of time T with N samplings. Thus, we first define a cost function

$$J_i = E \left\{ \frac{1}{2} \sum_{k=0}^{N-1} \left[\tilde{\mathbf{x}}_i^T(k) \mathbf{Q}_i \tilde{\mathbf{x}}_i(k) + u_i(k) r_i u_i(k) \right] \right\} \tag{29}$$

where $E\{\cdot\}$ is the expectation for a variable and $\mathbf{Q}_i = \begin{bmatrix} \rho_i^{ss} & 0 \\ 0 & \rho_i^{l\min} \end{bmatrix}$ and r_i are controlling weights, the values of which can be adjusted according to the control requirements. These weights determine whether or not the corresponding element is important since we can give more or less weight to any term in $\tilde{\mathbf{x}}_i(k) = \begin{bmatrix} \bar{\varepsilon}_i^{ss}(k), \varepsilon_i^{l\min}(k) \end{bmatrix}^T$ and $u_i(k)$. Specifically, ρ_i^{ss} and $\rho_i^{l\min}$ help us to pay more attention to the SINR and the IT threshold tracking in particular, and r_i can limit the energy of the controller. Since the SU should efficiently utilize the available spectrum resources, we assign to $\rho_i^{l\min}$ a value larger than that of ρ_i^{ss} and r_i to achieve better tracking of the IT *a priori*.

Interestingly, we know that (29) subject to (28) is a linear quadratic optimal control problem. However, we cannot directly use a linear quadratic regulator (LQR) to solve this problem because the fluctuation term $\tilde{\mathbf{w}}_i(k)$ in (28) is considered as exogenous input. For this optimal control problem, how much information regarding this exogenous input is available *a priori* will determine the control mode and precision [16], [18]. If the stochastic distribution of the exogenous disturbance is assumed to be the zero-mean white Gaussian sequence, the controller can be formulated as an LQG solution; otherwise, a more complex stochastic control theory should be introduced, such as $\mathcal{H}_\infty$ control technology which has been studied in our follow-up works. Here, we study the former case to show the effectiveness of power allocation via our control method in this CRN in contrast to using optimization approaches. We assume that $\tilde{\mathbf{w}}_i(k)$ is a 2×1 random vector with a covariance matrix, as follows:

$$\mathbf{Q}_i^{\mathbf{w}} = E \left\{ \tilde{\mathbf{w}}_i(k) \tilde{\mathbf{w}}_i^T(k) \right\} = \begin{bmatrix} \sigma_{\bar{\omega}_{\mu_i}}^2 & 0 \\ 0 & \sigma_{\bar{\omega}_{h_i}^{l\min}}^2 \end{bmatrix} \tag{30}$$

In the LQG regulator design, the output measurement must be considered, which is written as a linear function with state

$$\begin{bmatrix} \mathbf{B}_i^2 & \mathbf{A}_i \mathbf{B}_i^2 & \cdots & \mathbf{A}_i^L \mathbf{B}_i^2 \end{bmatrix} = \begin{bmatrix} 1 & 1-\alpha_i & (1-\alpha_i)^2 & \cdots & (1-\alpha_i)^L \\ 0 & -\alpha_i & -2\alpha_i + \alpha_i^2 & \cdots & (1-\alpha_i)^L - 1 \\ \vdots & \vdots & \vdots & \ddots & \vdots \\ 0 & -\alpha_i & -2\alpha_i + \alpha_i^2 & \cdots & (1-\alpha_i)^L - 1 \end{bmatrix} \tag{26}$$
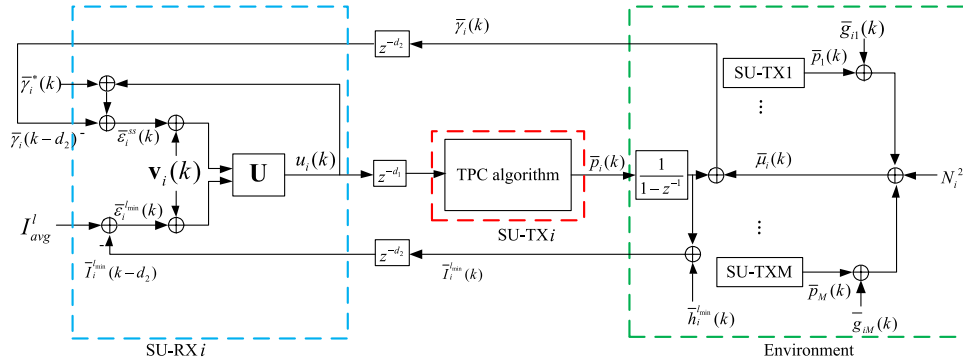
FIGURE 3. Closed-loop control system of distributed power allocation.

vector $\tilde{\mathbf{x}}_i(k)$ as

$$\mathbf{y}_i(k) = \mathbf{C}_i\tilde{\mathbf{x}}_i(k) + \mathbf{v}_i(k) \qquad (31)$$

where the coefficient matrix $\mathbf{C}_i$ is assumed to be a unit matrix and the measurement noise $\mathbf{v}_i(k)$ with the covariance matrix $\mathbf{R}_i^{\mathbf{v}} = E\left\{\mathbf{v}_i(k)\mathbf{v}_i^T(k)\right\}$ is independent of $\tilde{\mathbf{w}}_i(k)$.

Our power allocation based on the LQG regulator is such that we find a controller $u_i^*(k)$ that can minimize the stochastic quadratic cost function (29) subject to the state-space constraint (28). Moreover, this solution is in the form of measurement state feedback $u_i^*(k) = -\mathbf{K}_i\tilde{\mathbf{x}}_i(k)$, where $\mathbf{K}_i$ is the state feedback gain calculated based on the LQR solution [31]. The state variable used here can be replaced by the estimate $\hat{\mathbf{x}}_i(k)$ from the relevant Kalman filter. The simplest way to obtain an LQG regulator is to calculate a stable state controller with the assumption that N approaches infinity for one calculation of $\mathbf{K}_i$. This solution is often called the infinite domain solution.

With the initial predicted value $\hat{\mathbf{x}}_i(0) = \mathbf{0}$ and $\mathbf{P}_i^K(0) = E\left\{\tilde{\mathbf{x}}_i(0)\tilde{\mathbf{x}}_i^T(0)\right\}$, $u_i^*(k)$ is calculated by iteration for all $k > 0$, with

$$\mathbf{K}_i = \left[r_i + \left(\tilde{\mathbf{B}}_i^2\right)^T\mathbf{P}_i\tilde{\mathbf{B}}_i^2\right]^{-1}\left(\tilde{\mathbf{B}}_i^2\right)^T\mathbf{P}_i\tilde{\mathbf{A}}_i \qquad (32)$$

$$u_i^*(k) = -\mathbf{K}_i\hat{\mathbf{x}}_i(k) \qquad (33)$$

$$\mathbf{L}_i = \tilde{\mathbf{A}}_i^T\mathbf{P}_i^K\mathbf{C}_i^T\left[\mathbf{R}_i^{\mathbf{v}} + \mathbf{C}_i\mathbf{P}_i^K\mathbf{C}_i^T\right]^{-1} \qquad (34)$$

where $\hat{\mathbf{x}}_i(k)$ is defined as (35), as shown at the bottom of the next page, $\mathbf{P}_i$ and $\mathbf{P}_i^K(k+1)$ are calculated by using the discrete-time algebra Riccati equation (36), as shown at the bottom of the next page, and its recursive form (37), as shown at the bottom of the next page, respectively. Specifically, the former runs forward in time to calculate the optimal control gain $\mathbf{K}_i$, while the latter runs backward in time to estimate the instant value of the state vector. Therefore, a closed-loop distributed power control scheme, with $u_i^*(k)$ added to (13) to adjust the target-SINR for the CRN, is given as

$$\begin{aligned}\bar{p}_i(k+1) &= \bar{p}_i(k) + \alpha_i\left[\bar{\gamma}_i^*(k-1) + u_i^*(k-1) - \bar{\gamma}_i(k)\right]\\ &= \bar{p}_i(k) + \alpha_i\left[\bar{\gamma}_i^*(k-1) - \bar{\gamma}_i(k)\right] + \alpha_iu_i^*(k-1)\end{aligned} \qquad (38)$$

The corresponding closed-loop controlled system diagram is given in Fig. 3.

From (38), we can find that the control algorithm has a time delay of one sample. From Fig. 3, we also know that there is another kind of time delay in the closed-loop control system [32]. Briefly speaking, it takes some time before a calculated power is actually used and its effect is observed by others. Additional delays are caused by the fact that power update commands are allowed to be transmitted only at certain instances in time. In addition, the measuring procedure also takes time, and the measurement results are sent to the power control algorithm at certain instances in time. In total, we can divide the whole delay d into two delays: forward delay d_1, which includes the sample delay, and feedback delay d_2, with $d = d_1 + d_2$. Although the most recently computed output power levels are not immediately reflected in the measurements, resulting in delayed feedback information, these power levels can still be used to adjust the measurements accordingly. To simplify the controller design, we use the approach proposed in [32] to compensate for the time delay, i.e.,

$$\breve{\gamma}_i(k) = \bar{\gamma}_i(k) + \bar{p}_i(k) - \bar{p}_i(k-d) \qquad (39)$$

is introduced to measure the target-SINR. Other compensation methods for the time delay can also be adopted, such as reconstruction of an augmented state-space model with a new state vector $\mathbf{X} = \left[\tilde{\mathbf{x}}_i^T(k)\ u_i(k-d)\ \cdots\ u_i(k-1)\right]^T$ and the design of an optimal controller [33].

Using (38), we can realize the power allocation for an SU in the given CRN. However, we should note that there are some concerns regarding this original proposed control algorithm: (i) It is established on the basis of the hypothesis that each SU can satisfy its own minimal communication requirement if $\bar{\gamma}_i(k)$ reaches $\bar{\gamma}_i^*(k)$. (ii) The interference affecting the PU can sometimes be greater than the IT threshold because of the existence of exogenous input $\tilde{\mathbf{w}}_i(k)$ and the measurement noise $\mathbf{v}_i(k)$. (iii) The control parameters do not change with the communication situation in time. To address these considerations, we modify the above control algorithm and obtain an improved power control scheme.

IV. TIME-VARYING CONTROLLER WITH ADAPTIVE WEIGHT AND SAFETY MARGIN SWITCHING SCHEME

In this section, we introduce the adaptive weight and safety margin switching scheme for the IT threshold. Both are developed to enhance the QoS of communication.

In a communication system, the essential measure of QoS is the SINR related to all performance indexes, such as the data transmission rate, BER, etc. Here, we denote the data transmission rate as a Shannon capacity-like expression. Moreover, we introduce a lower bound and an upper bound of the SINR to ensure acceptable transmission, defined as $\gamma_i^{\min}$ and $\gamma_i^{\max}$, respectively. Then, according to [19], the relationship among the data transmission rate, the instantaneous SINR and the threshold of the SINR can be formulated as

$$R_i = \begin{cases} 0, & \gamma_i < \gamma_i^{\min} \\ W_B \log_2(1 + \gamma_i), & \gamma_i^{\min} \le \gamma_i \le \gamma_i^{\max} \\ W_B \log_2(1 + \gamma_i^{\max}), & \gamma_i > \gamma_i^{\max} \end{cases} \quad (40)$$

where W_B is the transmission bandwidth.

From the definition of (40), we know that R_i monotonically increases with γ_i when it is in $[\gamma_i^{\min}, \gamma_i^{\max}]$, the communication breaks off when $\gamma_i < \gamma_i^{\min}$, and the increase in the SINR is meaningless after the instantaneous SINR surpasses the required maximum $\gamma_i^{\max}$. Based on this property, we should keep the instantaneous SINR within the reasonable region and larger than the acceptable minimum $\gamma_i^{\min}$. Clearly, any user will be dropped if its instantaneous SINR still cannot reach the minimum value after utilizing all control effort.

In Section III, the proposed power controller with a fixed parameter is based on the hypothesis that $\gamma_i^*(k)$ is larger than $\gamma_i^{\min}$. Considering the concern discussed above regarding the variation of the communication environment and communication QoS, we propose an adaptive operation within $[\bar{\gamma}_i^{\min}, \bar{\gamma}_i^{\max}]$ and the corresponding decibel values of $\gamma_i^{\min}$ and $\gamma_i^{\max}$, and we define $\bar{\gamma}_i^{\text{mid}}$ as the mid-value in $[\bar{\gamma}_i^{\min}, \bar{\gamma}_i^{\max}]$.

A. WEIGHT PARAMETER ADJUSTMENT

In Section III, we briefly discussed the function of weights in the control results. However, the emphasis on the tracking of the IT threshold should not be dominant all the time. In fact, it can be appropriately relaxed when the performance of the

SU is satisfactory. For this reason, we adjust the weights in real time according to the actual situation of the CRN. In the optimal control theory, obtaining a suitable adaptive weight depends on the nature and the behavior of the system, which can significantly improve the system performance. Therefore, we introduce an adaptive weight for $\rho_i^{l_{\min}}(k)$ to better control the transmit power of each SU. Here, we set $\rho_i^{ss}(k) = 1$ and $r_i(k) = 1$ and only adaptively update $\rho_i^{l_{\min}}(k)$ by

$$\rho_i^{l_{\min}}(k+1) = \max\left\{\epsilon, \rho_i^{l_{\min}}(k) + \ell\left[\bar{\gamma}_i^{\text{mid}} - \bar{\gamma}_i^*(k)\right]\right\} \quad (41)$$

where the small constant ϵ is used to ensure that $\rho_i^{l_{\min}}(k)$ to track the IT threshold; ℓ is the update step-size, which is used to keep the variation of $\rho_i^{l_{\min}}(k)$ at a reasonable order of magnitude between two time slots. Specifically, in (41), we define the mid-SINR of the ith SU $\bar{\gamma}_i^{\text{mid}}$ as a standard for the communication performance to guarantee nominal work of the SU, as previously discussed. When the evolved target-SINR is beyond $\bar{\gamma}_i^{\text{mid}}$, $\rho_i^{l_{\min}}(k)$ is reduced to relax the use of spectral resources by the SU. In contrast, an increase of $\rho_i^{l_{\min}}(k)$ will result in the use of more spectral resources by the SU to achieve better communication performance without influencing the PU. This operation can limit the obtained target-SINR such that it is not far away from the mid-SINR. With this adaptive weight, the control gain in each time slot is calculated. We still use an infinite domain solution for the calculation of $\mathbf{K}_i(k)$ with the updated weight $\rho_i^{l_{\min}}(k)$ in each time slot. The control gain can be modified from (32) by (42), as shown at the bottom of the this page, with the time-varying parameter $\mathbf{Q}_i(k) = \begin{bmatrix} \rho_i^{ss} & 0 \\ 0 & \rho_i^{l_{\min}}(k) \end{bmatrix}$. Then, the parameter of a backwards-time Riccati recursion is determined according to (43), as shown at the bottom of the this page.

Although this power allocation method can protect the PU from interference caused by the SU to a certain extent, we still hope to find a protection mechanism for the PU from the perspective of the interference, for example, the channel fluctuation.

B. SWITCHING OF SAFETY MARGIN FOR IT THRESHOLD

Since the actual channel has some uncertainties, the designed power control scheme based on the channel parameter estimation cannot always guarantee that the actual interference

$$\hat{\mathbf{x}}_i(k) = \tilde{\mathbf{A}}_i \hat{\mathbf{x}}_i(k-1) + \tilde{\mathbf{B}}_i^2 u_i(k-1) + \mathbf{L}_i(\mathbf{y}_i(k-1) - \mathbf{C}_i \hat{\mathbf{x}}_i(k-1)) \quad (35)$$

$$\mathbf{P}_i = \mathbf{Q}_i + \tilde{\mathbf{A}}_i^T \mathbf{P}_i \tilde{\mathbf{A}}_i - \tilde{\mathbf{A}}_i^T \mathbf{P}_i \tilde{\mathbf{B}}_i^2 [r_i + \left(\tilde{\mathbf{B}}_i^2\right)^T \mathbf{P}_i \tilde{\mathbf{B}}_i^2]^{-1} \left(\tilde{\mathbf{B}}_i^2\right)^T \mathbf{P}_i \tilde{\mathbf{A}}_i \quad (36)$$

$$\mathbf{P}_i^K(k+1) = \tilde{\mathbf{A}}_i \mathbf{P}_i^K(k) \tilde{\mathbf{A}}_i^T + \mathbf{Q}_i^{\mathbf{w}} - \tilde{\mathbf{A}}_i \mathbf{P}_i^K(k) \mathbf{C}_i^T \left[\mathbf{R}_i^{\mathbf{v}} + \mathbf{C}_i \mathbf{P}_i^K(k) \mathbf{C}_i^T\right]^{-1} \mathbf{C}_i \mathbf{P}_i^K(k) \tilde{\mathbf{A}}_i^T \quad (37)$$

$$\mathbf{K}_i(k) = \left[r_i(k) + \left(\tilde{\mathbf{B}}_i^2\right)^T \mathbf{P}_i(k+1) \tilde{\mathbf{B}}_i^2\right]^{-1} \left(\tilde{\mathbf{B}}_i^2\right)^T \mathbf{P}_i(k+1) \tilde{\mathbf{A}}_i \quad (42)$$

$$\mathbf{P}_i(k) = \mathbf{Q}_i(k) + \tilde{\mathbf{A}}_i^T \mathbf{P}_i(k+1) \tilde{\mathbf{A}}_i - \tilde{\mathbf{A}}_i^T \mathbf{P}_i(k+1) \tilde{\mathbf{B}}_i^2 [r_i(k) + \left(\tilde{\mathbf{B}}_i^2\right)^T \mathbf{P}_i(k+1) \tilde{\mathbf{B}}_i^2]^{-1} \left(\tilde{\mathbf{B}}_i^2\right)^T \mathbf{P}_i(k+1) \tilde{\mathbf{A}}_i \quad (43)$$
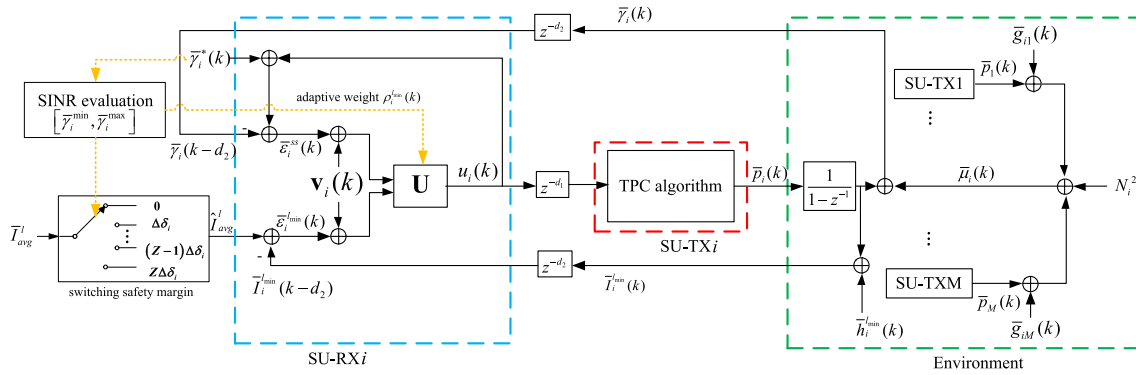
FIGURE 4. Closed-loop system of distributed power control based on LQG regulator with adaptive weight and switching scheme.

affecting the PU does not exceed the IT threshold. To further increase the possibility that the actual interference is below the IT threshold, we introduce a positive safety margin δ_i for the IT threshold. Then, the actual IT threshold is replaced by

$$\hat{I}_{avg}^l = \bar{I}_{avg}^l - \delta_i \qquad (44)$$

Clearly, each SU will use $\hat{I}_{avg}^l$ as a reference parameter to control the transmit power; thus, we should properly choose the margin δ_i.

As mentioned before, the required target-SINR in the interval from $\bar{\gamma}_i^{\min}$ to $\bar{\gamma}_i^{\max}$ can satisfy the communication requirement. Moreover, there is a connection between the SINR performance of the SU and the degree of interference with respect to the PU. To keep each SU from not allocating too much power after its performance is determined to be satisfactory, we should increase δ_i when $\bar{\gamma}_i^*(k)$ is higher than $\bar{\gamma}_i^{\max}$. This implies that we reduce the interference for both SUs and PUs. In contrast, when $\bar{\gamma}_i^*(k)$ is lower than $\bar{\gamma}_i^{\min}$, we should reduce δ_i to allocate more power to the SU to ensure better use of the spectrum resources.

According to the discussion above, we propose a switch scheme for updating δ_i. We assume that one unit change of δ_i is $\Delta\delta_i$, where $0 \leq \delta_i \leq Z\Delta\delta_i$ and Z is an integer given in advance according to the communication environment. This means that δ_i increases consecutively no more than Z times if the initial δ_i is zero. Then, the switching of δ_i for the IT threshold is performed as follows:

$$\delta_i = \begin{cases} \delta_i - \Delta\delta_i, & \bar{\gamma}_i^*(k) < \bar{\gamma}_i^{\min} \quad \text{and} \quad 0 < \delta_i \leq Z\Delta\delta_i \\ \delta_i + \Delta\delta_i, & \bar{\gamma}_i^*(k) \geq \bar{\gamma}_i^{\max} \quad \text{and } 0 \leq \delta_i < Z\Delta\delta_i \\ \delta_i, & \text{others} \end{cases} \qquad (45)$$

Note that any SU will be dropped if its communication performance is still not satisfactory when the corresponding safety margin reduces to zero.

In summary, each SU can control its transmit power according to the proposed algorithm using either the adaptive weight or via safety margin switching or both. To better understand our proposed distributed power allocation algorithm with the adaptive weight and safety margin switching, we present the entire closed-loop system in Fig. 4.

V. ANALYSIS OF THE PROPOSED ALGORITHM
In this section, we will conduct the analysis of the proposed algorithm in terms of the signal overhead, network stability, computational complexity and admission control.

A. SIGNAL OVERHEAD
In our power allocation scheme, we use the available information of the traditional power control algorithms for the traditional mobile communication networks, and we also require additional information. Specifically, in each time slot, when SUs update their transmit power, each SU needs to know the information regarding the difference between the IT threshold and the instantaneous interference from $\bar{\varepsilon}_i^l$ provided by the PU l. Therefore, our power allocation scheme needs a bit more signaling overhead than required in the traditional networks. This extra overhead is inevitable in CR systems, as the SU cannot achieve power control by itself without any help from the primary network and without disturbing the nominal communication of the PUs. For this reason, some approaches to transmit information from the primary network to each SU have been addressed. The authors of [24] propose setting the detection point in the primary network, which requires measuring the interference affecting PUs caused by SUs in real time and then sending the result as feedback to the SUs. In [34], the authors use the limited channel feedback technology to send the relevant primary network information.

When a PU transmits user information, the interference and the IT threshold can separately be transferred to each SU, or the difference between the interference and the IT threshold can be directly transmitted. Note that variation of the average IT threshold occurs only when the number of users in the secondary network changes, while the interference affecting the PU changes at every moment. Therefore, PUs are required to send as feedback both the real-time interference from the SUs in every time slot and the current average temperature threshold only when the number of SUs in the network changes. Undoubtedly, a PU can also choose to directly send feedback regarding the difference between the current IT threshold and the instantaneous interference affecting SUs. In practical applications, this information needs to

be quantified and transmitted via a feedback channel. We can determine which form of feedback information is appropriate according to the actual network situation.

B. SYSTEM STABILITY

When we put the state-space models of all SUs together, the whole dynamic system of the CRN can be expressed as in (46), as shown at the bottom of this page, where $\tilde{\mathbf{x}}_i(k) = \left[\bar{\varepsilon}_i^{ss}(k), \ \bar{\varepsilon}_i^{l\min}(k) \right]^T$ and $\tilde{\mathbf{w}}_i(k) = \left[\bar{\omega}_i(k), \ \bar{q}_i^{l\min}(k) \right]^T$, $i \in \mathcal{M}$ for each co-channel link. The entries of the corresponding matrices $\tilde{\mathbf{A}}_i$, $\tilde{\mathbf{B}}_i^1$ and $\tilde{\mathbf{B}}_i^1$ for $i \in \mathcal{M}$ are the same as those in (28). For the block diagonal decoupled system in (46), every subsystem for each co-channel link is equivalent to an independent system [19], [35]. The decentralized structure makes this decoupling possible because the influence of the co-channel is modeled as a steady first-order Markov random model via (10), as addressed in Section II. Since the network can be decomposed into M co-channel subsystems, the stability of the overall system is equal to that of each individual one. Thus, we can analyze the stability of the state-space model (28) to evaluate the entire stability of the CRN.

We briefly discuss the stability of (28). According to the control theory, we can deduce that (28) is internally stable if for the closed-loop system

$$\tilde{\mathbf{x}}_i(k+1) = \left(\tilde{\mathbf{A}}_i - \tilde{\mathbf{B}}_i^2 \mathbf{K}_i \right) \tilde{\mathbf{x}}_i(k) \qquad (47)$$

with zero input, the pair $\left(\tilde{\mathbf{A}}_i, \tilde{\mathbf{B}}_i^2 \right)$ is controllable, $\tilde{\mathbf{x}}_i(k)$ is detectable, and $\mathbf{Q}_i(k)$ is symmetric positive definite [36]. It is obvious that (47) is internally stable since these conditions are all satisfied. External stability, also called input-output stability, means that a bounded input always produces a bounded output. For a linear system, if its closed-loop system is controllable and observable, the external stability can be deduced by internal stability. In our control system, all the conditions mentioned above are available, thus we can conclude that system (46) is stable [19]. In general, the state feedback control structure of the proposed algorithm ensures the stability of the closed-loop system.

C. COMPUTATIONAL COMPLEXITY

It is worth mentioning that the complexity of our power allocation algorithm is very low compared to the algorithms based on optimization theory. In particular, for the static LQG control solution, the state feedback gain of infinite domain solutions $\mathbf{K}_i$ is calculated only one time due to the parameters being known. At the same time, all the matrices involved in the calculation have dimensions of 2×2, and these matrices, which need to be inversed, are converted into scalars. For the adaptive LQG power control scheme, the state feedback gain $\mathbf{K}_i$ is calculated in each time slot for the time-varying weight; this calculation is similar to the static LQG control solution. The difference is that $\mathbf{K}_i$ needs to be calculated at every moment.

D. ADMISSION CONTROL

To make the power control feasible, some central admission control should be added to the network to adjust the number of access users. This central admission control approach does not conform to the concept of our proposed distributed solutions. However, a distributed admission control is more suitable than the central one. In our scheme, we directly use the admission control method addressed in [19], where the user, who uses the maximum transmit power or for whom the interference affecting the PUs is above the IT threshold, fails to achieve the lowest acceptable SINR and thus automatically ends the communication.

VI. SIMULATION RESULTS

In this section, we present simulations to illustrate the performance of the proposed distributed power allocation scheme. We first consider a small-scale CRN for easy analysis of the overall performance. Then, we conduct simulations with more users to show the superiority of our power allocation based on LQG control compared with the conventional approaches. Note that our simulations are run only at the

$$
\begin{bmatrix} \tilde{\mathbf{x}}_1(k+1) \\ \vdots \\ \tilde{\mathbf{x}}_i(k+1) \\ \vdots \\ \tilde{\mathbf{x}}_M(k+1) \end{bmatrix} = \begin{bmatrix} \tilde{\mathbf{A}}_1 & 0 & \cdots & \cdots & 0 \\ 0 & \ddots & & & \vdots \\ \vdots & & \tilde{\mathbf{A}}_i & & \vdots \\ \vdots & & & \ddots & 0 \\ 0 & \cdots & \cdots & 0 & \tilde{\mathbf{A}}_M \end{bmatrix} \begin{bmatrix} \tilde{\mathbf{x}}_1(k) \\ \vdots \\ \tilde{\mathbf{x}}_i(k) \\ \vdots \\ \tilde{\mathbf{x}}_M(k) \end{bmatrix} + \begin{bmatrix} \tilde{\mathbf{B}}_1^1 & 0 & \cdots & \cdots & 0 \\ 0 & \ddots & & & \vdots \\ \vdots & & \tilde{\mathbf{B}}_i^1 & & \vdots \\ \vdots & & & \ddots & 0 \\ 0 & \cdots & \cdots & 0 & \tilde{\mathbf{B}}_M^1 \end{bmatrix} \begin{bmatrix} \tilde{\mathbf{w}}_1(k) \\ \vdots \\ \tilde{\mathbf{w}}_i(k) \\ \vdots \\ \tilde{\mathbf{w}}_M(k) \end{bmatrix}
$$

$$
+ \begin{bmatrix} \tilde{\mathbf{B}}_1^2 & 0 & \cdots & \cdots & 0 \\ 0 & \ddots & & & \vdots \\ \vdots & & \tilde{\mathbf{B}}_2^2 & & \vdots \\ \vdots & & & \ddots & 0 \\ 0 & \cdots & \cdots & 0 & \tilde{\mathbf{B}}_M^2 \end{bmatrix} \begin{bmatrix} u_1(k) \\ \vdots \\ u_i(k) \\ \vdots \\ u_M(k) \end{bmatrix} \qquad (46)
$$

frame level for the allocated transmit power and the interference without consideration of modulation and coding.

In each simulation scenario, we consider only the path loss and shadowing for all links regardless of fast fading, with the assumption that the period of power update is large enough for fast fading to occur, as mentioned in Section II. Thus, the coherent channel gain G_{ij} is assumed to follow a lognormal distribution

$$G_{ij} = G_0 \left(\frac{d_{ij}}{d_0} \right)^{-\eta} 10^{\frac{\psi_{dB}}{10}} \qquad (48)$$

where $G_0 = \left(\frac{\lambda}{4\pi d_0} \right)^2$ is a constant that depends on the antenna characteristics and the average channel attenuation, d_{ij} is the distance from the transmitter j to the receiver i, d_0 is a reference distance for the far-field antenna, η is the path loss exponent, which, depending on the physical environment, is set between 2 and 6, and ψ_{dB} is a Gaussian distribution random variable with zero-mean and variance $\sigma^2_{\psi_{dB}}$. The correlation between shadowing and distance can be characterized as

$$R(vT_s) = \sigma^2_{\psi_{dB}} a \qquad (49)$$

As discussed in Section II, $a = \exp\left(-\frac{vT_s}{X_s} \right)$, where the velocity v of each user approaches zero, resulting in $R(vT_s) = \sigma^2_{\psi_{dB}}$. These parameters can be obtained by approximating either the analytical or empirical model. In our simulations, we choose a carrier frequency f_c of 3 GHz ($\lambda = \frac{c}{f_c}$ and $c = 3 \times 10^8 m/s$), d_0 of 10 m, η of 4, $R(vT_s) = \sigma^2_{\psi_{dB}}$ of 3.65 and a transmission bandwidth W of 1 MHz.

Let us consider a small-scale CRN in which 2 PU-RXs and 3 SU-RXs are fixed and served by 1 PBS and 3 corresponding SU-TXs, respectively, in an area of 1000 m × 1000 m, as illustrated in Fig. 5(a), and a large-scale CRN in which 10 PU-RXs and 100 SU-RXs are fixed and served by 1 PBS and 100 corresponding SU-TXs, respectively, in an area of 10000 m × 10000 m, as illustrated in Fig. 5(b). The generalized background noise at each SU-RX is randomly generated among $(0, 1 \times 10^{-8})W$. The IT threshold of each PU is also taken randomly from an interval, where we take it from $(0, 1 \times 10^{-9})W$ and $(0, 1 \times 10^{-8})W$ in the first two parts and in the last part respectively. In these communication environments, each

SU-TX adjusts its transmit power by the proposed algorithm with a time delay of one sample.

A. ALGORITHM CONVERGENCE

We first verify the convergence of the algorithm with constant CSI where the channel gains do not change in the process of power control and without considering any measurement error and adaptive operations. Note that the LQG control becomes LQR control if we do not consider these factors. Thus, we set $\rho_i^{ss}(k) = 1$, $\rho_i^{l\min}(k) = 5$ and $r_i(k) = 1$. On the basis of these settings, the influence of standard target-SINR TPC gain α_i on IT threshold tracking and SINR tracking is shown in Fig. 6 and Fig. 7, respectively. From the two figures, we find that the ultimate interference power and SINR of each SU are the same no matter what the value of α_i is. However, different α_i results in different convergence rates, and larger α_i results in quicker convergence. Moreover, we cannot pursue only the convergence speed even though a high α_i will result in a large power increment in each time slot, which raises the interference from the SU to the PU above the average IT threshold (Ave-Ith). We can also see the
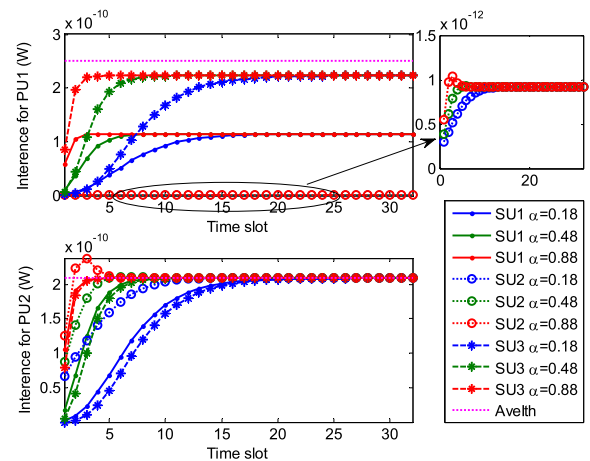
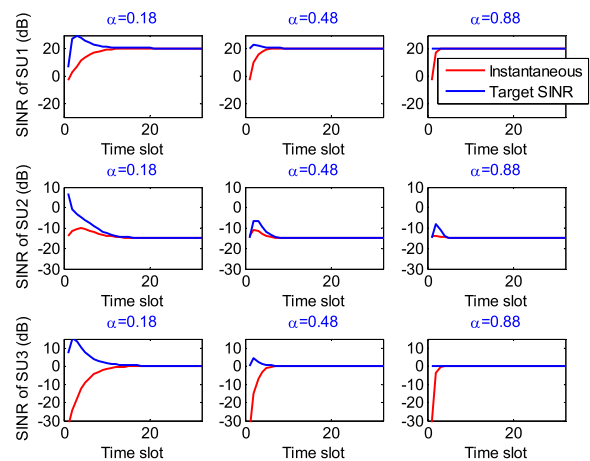**FIGURE 6.** IT threshold tracking versus difference α_i for each SU.

FIGURE 5. Placement of users. (a) Small-scale CRN. (b) Large-scale CRN.

FIGURE 7. SINR tracking versus difference α_i for each SU.

overshoot (the excessive interference affecting PU) in Fig. 6 when $\alpha_i = 0.88$. This means that α_i should be appropriately selected according to the practical communication situation. It is clear that this temporary excessive interference occurs only in the first few time slots, while the interference power affecting the PU is not larger than the average IT threshold after several transition time slots.

B. PERFORMANCE OF THE PROPOSED ALGORITHMS WITH TIME-VARYING CSI

We give the time response of the closed-loop power control system for time-varying CSI to illustrate the effectiveness of our power allocation algorithm based on the LQG regulator. As shown in Section II, the channel gain of each link at the decibel scale is formulated as a first-order Markov process of the white Gaussian fluctuation with zero-mean and a variance of 0.02. We also assume that the measurement error of the state variables is the white Gaussian sequence with zero-mean and a variance of 1. We give the response curves of the closed-loop power control system with the LQR and the LQG regulator in Fig. 8. To demonstrate the steady-state response, we extend the number of control time slots to 100.

From Fig. 8, we see that the control performance with the LQR is worse than that with the LQG regulator for the stochastic channel in three aspects, namely, power evolution, interference tracking and target-SINR tracking. Specifically, looking at the evolution of the transmit power, the tracking of the average IT threshold or the tracking of the target-SINR, we find that the response of the LQR varies greatly compared with that of the LQG regulator because as the channel state evolves over time, the LQG regulator has strong robustness with respect to the actual channel variation. However, the values corresponding to the LQR fluctuate around those corresponding to the LQG regulator, showing that the proposed algorithm has robustness whether or not we carry out Kalman estimation.

C. PERFORMANCE COMPARISON OF DIFFERENT ALGORITHMS

Now, we compare the performance of our proposed algorithm with that of typical power allocation algorithms for CRNs, namely, the distributed optimization algorithm (referred to as ConOpt algorithm) and TPC-PP and ITPC-PP algorithms in [26]. In ConOpt algorithm, the objective is to maximize the total data transmission rate of SUs with the IT constraint on each PU and the maximum transmit power constraint. However, the chosen feasible region for this problem makes the IT constraint dominant and the maximum transmit power constraint weaker. Similar to our proposed scheme, TPC-PP and ITPC-PP algorithms are also designed on the basis of TPC algorithm, where each SU employs TPC algorithm as long as the total interference power at each PU-RX is below a given IT threshold. Otherwise, they will reduce the transmit power in proportion to a ratio calculated according to the relationship between the given threshold and the total interference power at PU-RX. In particular, for our

communication scenario, the ratio used by TPC-PP algorithm can be expressed as

$$\beta_i(k) = \min_l \left\{ \frac{I_{th}^l}{\sum_{i \in \mathcal{M}} h_i^l(k) p_i(k)} \right\}, \quad l \in \mathcal{L} \quad (50)$$

And the ratio used by ITPC-PP algorithm can be written as

$$\tilde{\beta}_i(k) = \begin{cases} \beta_i(k), & \text{if } \beta_i(k) \geq 1 \\ \beta_i(k) \left(\left| I_{th}^{l_{\min}} - I^{l_{\min}} \right| \frac{I^{l_{\min}} - I_i^{l_{\min}}}{h_i^{l_{\min}}} \right), & \text{others} \end{cases} \quad (51)$$

where $I^{l_{\min}} = \sum_{i \in \mathcal{M}} h_i^{l_{\min}}(k) p_i(k)$ and $I_i^{l_{\min}} = h_i^{l_{\min}}(k) p_i(k)$. From (50) and (51), we can find that ITPC-PP algorithm considers the interference level of PUs from each SU further comparing with that of TPC-PP algorithm.

We compare the performances of these algorithms for the small-scale CRN given in Fig. 5(a) and the large-scale CRN shown in Fig. 5(b) in consideration of both constant CSI and time-varying CSI. In the former case, the channel gains do not change in the power control process and the measurement error of the required information is also not considered. In the time-varying CSI case, each channel gain changes following the previous description in (48), and the measurement error of the required information is considered. The average performance comparison, conducted via 1000 Monte Carlo experiments using randomly generated large-scale CRN snapshots, is also given. We compare the interference for each PU, the outage ratio of PUs and SUs, and the total data transmission rates of SUs respectively. In the simulations, the outage ratio of PUs is defined as the ratio of the number of PUs whose IT threshold is broken to the total number of PUs. The outage ratio of SUs is defined as the ratio of the number of SUs whose instantaneous SINR is lower than the fixed target-SINR to the total number of active SUs.

Note that the outage ratio used is the mean of the ratios of the last 15 time slots for the fixed 0 *dB* target-SINR in the following first two parts. The total data transmission rate is the sum of the data transmission rates of all SUs, defined as (40).

1) SMALL-SCALE CRN WITH CONSTANT CSI

First, we present the performance of these algorithms for constant CSI which is an ideal situation always considered in the analysis of the previous power allocation algorithms. In this case, we compare LQR algorithm with ConOpt, TPC-PP and ITPC-PP algorithms.

Fig. 9 illustrates the interference to the 1st PU and the 2nd PU, where Ith1 and Ith2 are the IT thresholds of the 1st PU and the 2nd PU, respectively. From Fig. 9, we observe that, in this ideal situation, all algorithms can keep the IT threshold of each PU as they are all designed under the IT constraint. Fig. 9 also shows that the interference from SUs to each PU is almost the same for ConOpt algorithm since this algorithm considers all PUs equally. In contrast, this interference
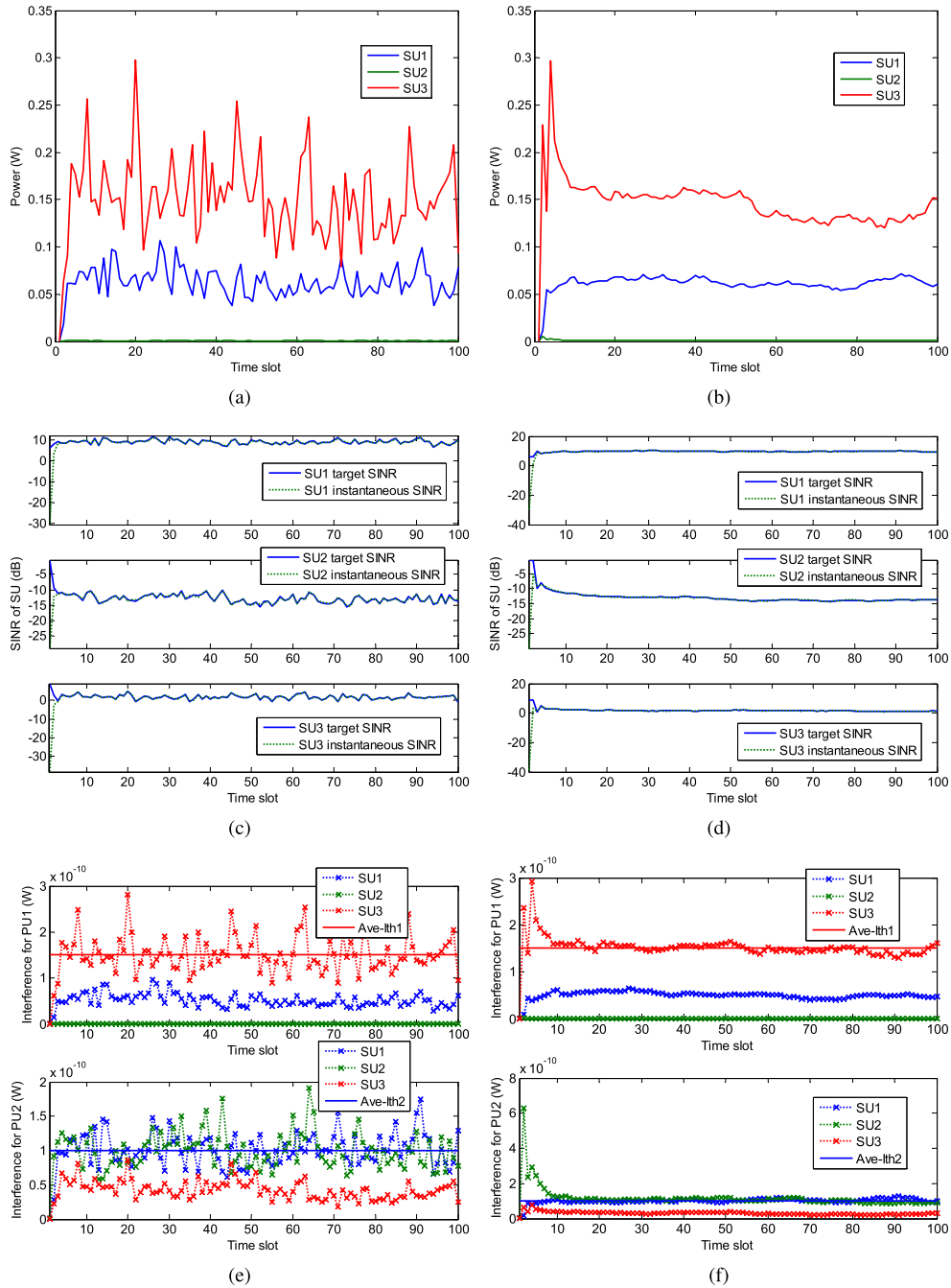
FIGURE 8. Performance comparison of different algorithms with time-varying CSI. (a) by LQR control. (b) by LQG control. (c) by LQR control. (d) by LQG control. (e) by LQR control. (f) by LQG control.

produced by TPC-PP algorithm, ITPC-PP algorithm and our proposed algorithm is more serious for the 2nd PU, as these three algorithms pay more attention to the most vulnerable PU. As shown in Fig. 9, for the 2nd PU, the resulting interference of either TPC-PP or ITPC-PP algorithms is larger than that of our algorithm, and it even reaches the IT threshold of the 2nd PU, which implies the conservativeness of the average IT constraint used. Meanwhile, the use of the average IT constraint makes the interference affecting any PU not

very high. In addition, we note that the results of TPC-PP algorithm and ITPC-PP algorithm are almost the same since $\beta_i(k) \geq 1$ always holds in this case. From (50) and (51), we can see that the two algorithms execute different control laws only when $\beta_i(k) < 1$.

Fig. 10 shows the outage ratios for PUs and SUs. We can see that ConOpt algorithm, TPC-PP algorithm, TPC-PP algorithm and our algorithm do not allow the communication interruption of PU, which means that the four algorithms are
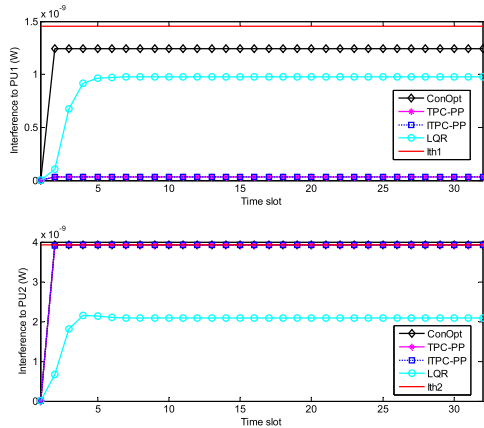
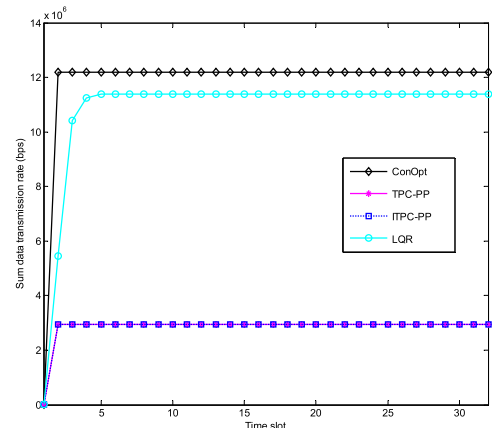**FIGURE 9.** Total interference from SUs to PU for different algorithms.

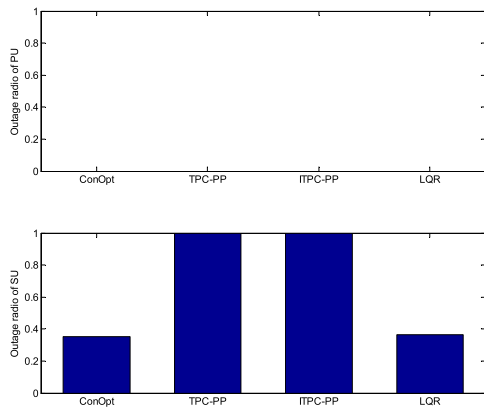**FIGURE 11.** Total transmission rate of SUs for different algorithms.

FIGURE 10. Outage ratio of PUs and SUs for different algorithms.

effective to protect PUs in the ideal situation. We find that the outage ratio of SUs by our algorithm is almost the same as that by ConOpt algorithm and lower than those by both TPC-PP and ITPC-PP algorithms when we guarantee a zero outage ratio for PUs.

The total data transmission rate of SUs is given in Fig. 11. It shows that the total data transmission rate of ConOpt algorithm is the highest among these algorithms. The reason is that it takes the total data transmission rate of SUs as the optimization objective under the condition that the communication of PU cannot be broken. From this figure, we also find that the proposed LQR algorithm cannot achieve such a high transmission rate, while it can give reliable protection to PUs and performs similarly as ConOpt algorithm and better than TPC-PP and ITPC-PP algorithms. Moreover, the total data transmission rates of TPC-PP algorithm and ITPC-PP algorithm are still the same since the IT threshold of each PU is never broken in the control process to hold $\beta_i(k) \geq 1$.

2) SMALL-SCALE CRN WITH TIME-VARYING CSI
For the time-varying CSI in the period of data packet transmission, SUs use the LQG regulator to control power in our proposed scheme. To conduct the simulation we take the corresponding robust versions of ConOpt, TPC-PP and

ITPC-PP algorithms, called WorstCase, TPC-PP-W and ITPC-PP-W respectively. These robust algorithms are all based on the robust optimization theory [10], [11], [26], where a worst percentage of uncertainty P_δ is assumed to deal with all factors that are unsatisfactory but inevitable, such as the fluctuation of channel gain, the measurement error of the required signal and the influence caused by time delay of the feedback information in the power control process. In fact, a high worst percentage of uncertainty can reduce the sensitivity of a power allocation algorithm to these undesirable factors but enhance the conservativeness of the algorithm. In the following simulations, we use three typical worst percentages of uncertainty, namely 0.05, 0.1 and 0.2, by which the corresponding simulation results are illustrated in Fig. 12, Fig. 13 and Fig. 14 respectively.
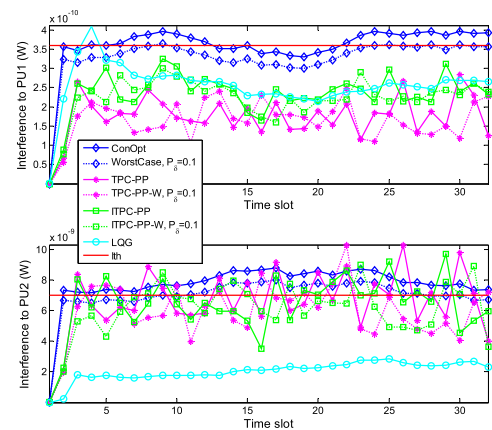

FIGURE 12. Total interference from SUs to PU for different algorithms.

As shown in Fig. 12, due to the existence of the channel variation and the measurement error, there are interference fluctuations for all algorithms. Except for our algorithm, the interferences affecting PUs, especially PU2, from all other algorithms exceed the corresponding IT threshold more times. Although the corresponding robust versions of ConOpt, TPC-PP and ITPC-PP algorithms outperform
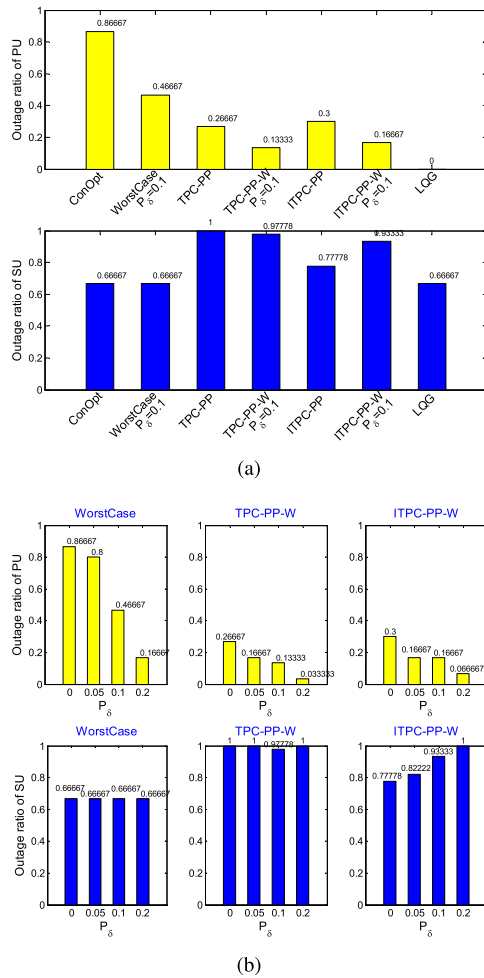
FIGURE 13. Outage radio of PUs and SUs for different algorithms. (a) Outage radio. (b) Outage radio verse uncertainty percentage.

the original versions in this matter, they still have much more stronger interference to PUs than our algorithm with LQG regulator which has only slightly higher interference affecting the 1st PU in the first few control transient slots. After this period, the interference becomes smooth compared with those of other algorithms due to the control process, and the interference affecting PUs is always below the IT threshold.

In order to demonstrate the superiority of our proposed scheme and the effect of different worst percentages of the uncertainty used, we give the bar graphs of outage radio of PUs and SUs for different algorithms and different worst percentages of uncertainty in Fig. 13.

Fig. 13(a) presents the outage radio of PUs and SUs for different algorithms in the power control process, where the worst percentage of uncertainty adopted by WorstCase, TPC-PP-W and ITPC-PP-W algorithms is 0.1. In the process, we find that only our LQG algorithm can guarantee zero outage ratio of PUs. On the contrary, the other algorithms disturb PUs more or less. Additionally, it not only protects the normal communication of PUs but also obtains similar outage ratio of SUs as ConOpt and WorstCase algorithms. Although the

WorstCase, TPC-PP-W and ITPC-PP-W algorithms take 0.1 worst percentage of uncertainty to protect PUs, their outage ratios of PUs are still over zero. In addition, from Fig. 13(a), we also obverse that ITPC-PP algorithm and its robust version, ITPC-PP-W algorithm, can obtain a better outage ratio of SUs than that of TPC-PP and TPC-PP-W algorithms respectively, which is consistent with the results in [26]. We also find that the outage ratio of PUs of ITPC-PP-W algorithm is lower than that of ITPC-PP algorithm, but its outage ratio of SUs is higher compared with that of ITPC-PP algorithm. The reason is that outage ratios of PUs and SUs are in contradiction to each other.

We use Fig. 13(b) to describe the effect of different worst percentages of uncertainty. As addressed in [10] and [11], the original non-robust algorithm is equivalent to the robust algorithm with zero worst percentage of uncertainty, we give the comparison of WorstCase, TPC-PP-W and ITPC-PP-W algorithms with $P_\delta = 0$, $P_\delta = 0.05$, $P_\delta = 0.1$ and $P_\delta = 0.2$ respectively. As described above, a high worst percentage of uncertainty will introduce strong conservativeness. Thus, for these algorithms, the higher the worst percentage of uncertainty they use, the lower the outage ratio of PUs they get or the larger the outage ratio of SUs they obtain. In general, the protection for PUs using the robust algorithm depends on the priori knowledge regarding to the worst percentage of uncertainty. However, because of the randomness of the channel fluctuation and the measurement error of the required information, the significant tendency in the simulation is obvious but slightly variable; such as the outage ratio of SUs obtained by TPC-PP-W algorithm with 0.1 percentage of uncertainty is little lower than that of other uncertainties.

In Fig. 14, we present the total data transmission rate of SUs for above algorithm. This performance corresponding to the LQG regulator is still between those of ConOpt algorithm and TPC-PP and ITPC-PP algorithms including their robust versions. The smoothness of the transmission rate of the LQG regulator is nearly the same as that of WorstCase
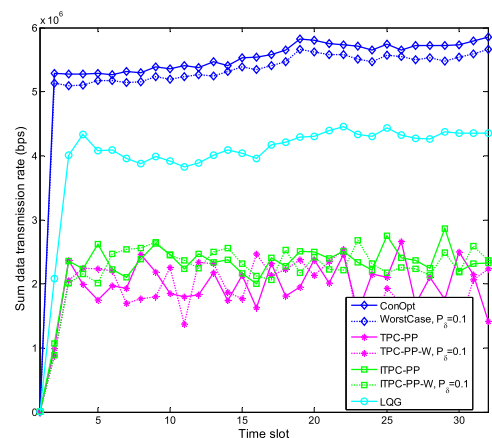

FIGURE 14. Total transmission rate of SUs for different algorithms.

algorithm but the protection for PUs is much better than that of WorstCase algorithm, which is the most important requirement in a CRN. From this figure, we also know that ITPC-PP algorithm can get higher total transmission rate of SUs than that of TPC-PP algorithm since it uses the control law (51) to further deal with the interference level of PUs from each SU.

3) LARGE-SCALE CRN WITH TIME-VARYING CSI

Now we consider a large-scale CRN in the simulations with time-varying channel gain of each link. In this scenario, we adopt the time-varying controller having an adaptive weight and switching safety margin of the IT threshold proposed in Section IV, with $\epsilon = 2$, $\ell = 1 \times 10^{-3}$ and $\rho_i^{l\min} = 5$ for each SU, $\Delta\delta = 1$, the largest number of Z being 20, and the initial safety margin for each SU being 5. In the following figures, we illustrate the performance of different algorithms with different fixed target-SINRs $[-15, -5, 0, 5, 10, 20, 30]$ dB, where the fixed target-SINR is the mid-value $\bar{\gamma}_i^{\mathrm{mid}}$ in $\left[\bar{\gamma}_i^{\min}, \bar{\gamma}_i^{\max}\right]$, with $\bar{\gamma}_i^{\max} - \bar{\gamma}_i^{\min} = 40$ dB. In addition, the performance simulations of the power allocation with the time-varying controller are similar to those in Fig. 6 ~Fig. 14.

Fig. 15 gives the outage ratios of both PUs and SUs for different algorithms versus the fixed target-SINR in the large-scale CRN as shown in Fig. 5(b). The results are the average value of 1000 times experiments. We find that WorstCase, TPC-PP-W and ITPC-PP-W algorithms with 0.1 worst percentage of uncertainty perform better than ConOpt, TPC-PP and ITPC-PP algorithms respectively, but they cannot guarantee zero outage ratios for PU, and our proposed algorithm performs the best. From Fig. 15, we also find that the outage ratios of PU produced by ConOpt and WorstCase algorithms do not change with the variation of the fixed target-SINR, since they only maximize the current total data transmission rate without considering the lowest acceptable SINR. Moreover, our algorithm has almost the same the outage ratio of SUs as that of WorstCase algorithm.
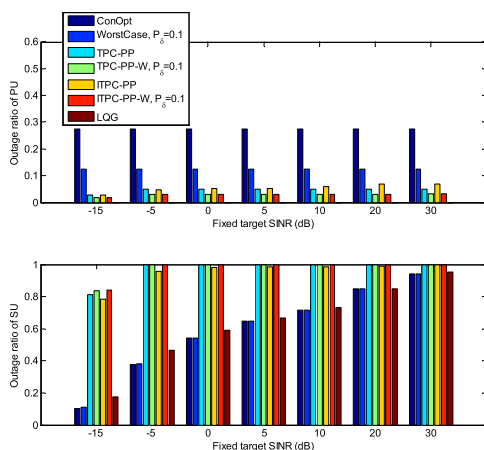
In Fig. 16, we present the average outage ratio versus the fixed target-SINR from 1000 independent snapshots for the large-scale CRN where the location of each user is randomly generated and the worst percentage of uncertainty used by WorstCase,TPC-PP-W and ITPC-PP-W algorithms is 0.2. We find that our LQG regulator ensures a zero outage ratio no matter what the fixed target-SINR is for PUs, but the other algorithms cannot. In addition, our scheme has almost the same SU outage ratio as those of ConOpt and WorstCase algorithms but lower than those of TPC-PP, TPC-PP-W, ITPC-PP and ITPC-PP-W algorithms.
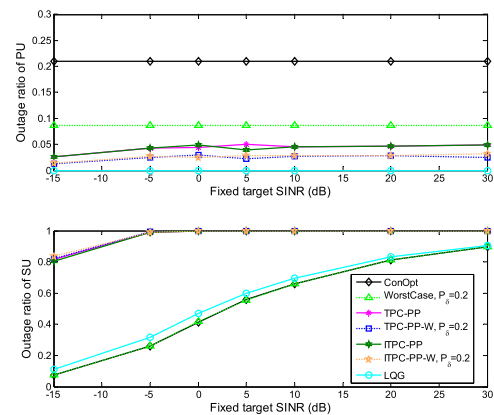

FIGURE 16. Average outage ratio for PUs and SUs versus fixed target-SINR for different algorithms in a large-scale CRN.

VII. CONCLUSIONS

We propose a distributed closed-loop power allocation algorithm and its improved version with adaptive weight adjustment and a safety switching mechanism for CRNs, where the power control problem is formulated by a state-space description instead of using optimization approaches. This proposed algorithm based on the dynamic description of the problem can well guarantee a zero outage ratio for PUs and an acceptable outage ratio and a total data transmission rate for SUs when the channel gain varies. In addition, this power control algorithm achieves the same signal overhead as those of the previous power allocation algorithms while also having a lower computational complexity for a time-varying channel. Compared with the power allocation algorithms based on convex optimization technology, this kind of power allocation is much more practical since the whole CRN is considered as a closed-loop system with a changing environment and uncertainty. Based on the given simulation results from different perspectives, we can conclude that the proposed power allocation method has more advantages; thus, it will be developed further for more complicated CRNs. Finally, we believe that dynamic control for CRNs with dynamic descriptions is more interesting and challenging since this work can address many dynamic factors, such as a time-varying channel, stochastic uncertainty, different estimation errors, time delay, the random changing of users, different QoS requirements, robustness against control parameters, etc.


FIGURE 15. Outage ratio for PUs and SUs versus fixed target-SINR for different algorithms.

REFERENCES

[1] S. Haykin, "Cognitive radio: Brain-empowered wireless communications," *IEEE J. Sel. Areas Commun.*, vol. 23, no. 2, pp. 201–220, Feb. 2005.

[2] X. Kang, H. K. Garg, Y.-C. Liang, and R. Zhang, "Optimal power allocation for OFDM-based cognitive radio with new primary transmission protection criteria," *IEEE Trans. Wireless Commun.*, vol. 9, no. 6, pp. 2066–2075, Jun. 2010.

[3] G. Bansal, M. J. Hossain, and V. K. Bhargava, "Adaptive power loading for OFDM-based cognitive radio systems with statistical interference constraint," *IEEE Trans. Wireless Commun.*, vol. 10, no. 9, pp. 2786–2791, Sep. 2011.

[4] Z. Guan, T. Melodia, D. Yuan, and D. A. Pados, "Distributed resource management for cognitive ad hoc networks with cooperative relays," *IEEE/ACM Trans. Netw.*, vol. 24, no. 3, pp. 1675–1689, Jun. 2016.

[5] T. Li, N. B. Mandayam, and A. Reznik, "A framework for distributed resource allocation and admission control in a cognitive digital home," *IEEE Trans. Wireless Commun.*, vol. 12, no. 3, pp. 984–995, Mar. 2013.

[6] M. R. Javan and A. R. Sharafat, "Distributed joint resource allocation in primary and cognitive wireless networks," *IEEE Trans. Commun.*, vol. 61, no. 5, pp. 1708–1719, May 2013.

[7] P. Setoodeh and S. Haykin, "Robust transmit power control for cognitive radio," *Proc. IEEE*, vol. 97, no. 5, pp. 915–939, May 2009.

[8] J. Tadrous, A. Sultan, and M. Nafie, "Admission and power control for spectrum sharing cognitive radio networks," *IEEE Trans. Wireless Commun.*, vol. 10, no. 6, pp. 1945–1955, Jun. 2011.

[9] M. H. Islam, Y.-C. Liang, and A. T. Hoang, "Distributed power and admission control for cognitive radio networks using antenna arrays," in *Proc. 2nd IEEE Int. Symp. New Frontiers Dyn. Spectr. Access Netw.*, Dublin, Ireland, Apr. 2007, pp. 250–253.

[10] S. Parsaeefard and A. R. Sharafat, "Robust distributed power control in cognitive radio networks," *IEEE Trans. Mobile Comput.*, vol. 12, no. 4, pp. 609–620, Apr. 2013.

[11] Y. Xu, X. Zhao, and Y.-C. Liang, "Robust power control and beamforming in cognitive radio networks: A survey," *IEEE Commun. Surveys Tuts.*, vol. 17, no. 4, pp. 1834–1857, 4th Quart., 2015.

[12] C. Luo, G. Min, F. R. Yu, M. Chen, L. T. Yang, and V. C. M. Leung, "Energy-efficient distributed relay and power control in cognitive radio cooperative communications," *IEEE J. Sel. Areas Commun.*, vol. 31, no. 11, pp. 2442–2452, Nov. 2013.

[13] M. Cui, B.-J. Hu, X. Li, H. Chen, S. Hu, and Y. Wang, "Energy-efficient power control algorithms in massive MIMO cognitive radio networks," *IEEE Access*, vol. 5, pp. 1164–1177, 2017.

[14] F. Foukalas, R. Shakeri, and T. Khattab, "Distributed power allocation for multi-flow carrier aggregation in heterogeneous cognitive cellular networks," *IEEE Trans. Wireless Commun.*, vol. 17, no. 4, pp. 2486–2498, Apr. 2018.

[15] B. Li, Z. Fei, Z. Chu, F. Zhou, K.-K. Wong, and P. Xiao, "Robust chance-constrained secure transmission for cognitive satellite–terrestrial networks," *IEEE Trans. Veh. Technol.*, vol. 67, no. 5, pp. 4208–4219, May 2018.

[16] A. Subramanian and A. H. Sayed, "Joint rate and power control algorithms for wireless networks," *IEEE Trans. Signal Process.*, vol. 53, no. 11, pp. 4204–4214, Nov. 2005.

[17] L. Qian and Z. Gajic, "Variance minimization stochastic power control in CDMA systems," *IEEE Trans. Wireless Commun.*, vol. 5, no. 1, pp. 193–202, Jan. 2006.

[18] N. U. Hassan, M. Assaad, and H. Tembine, "Distributed H∞-based power control in a dynamic wireless network environment," *IEEE Commun. Lett.*, vol. 17, no. 6, pp. 1124–1127, Apr. 2013.

[19] F. de Sousa Chaves, M. Abbas-Turki, H. Abou-Kandil, and J. M. T. Romano, "Transmission power control for opportunistic QoS provision in wireless networks," *IEEE Trans. Control Syst. Technol.*, vol. 21, no. 2, pp. 315–331, Mar. 2013.

[20] N. U. Hassan and M. Assaad, "Dynamic resource allocation in multiservice OFDMA systems with dynamic queue control," *IEEE Trans. Commun.*, vol. 59, no. 6, pp. 1664–1674, Jun. 2011.

[21] R. Qian, Z. Duan, and Y. Qi, "Stability of power control in multiple coexisting wireless networks: An $\mathcal{L}_2$ small-gain perspective," *IEEE Trans. Circuits Syst. I, Reg. Papers*, vol. 64, no. 5, pp. 1235–1246, May 2017.

[22] S. Haykin and P. Setoodeh, "Cognitive radio networks: The spectrum supply chain paradigm," *IEEE Trans. Cogn. Commun. Netw.*, vol. 1, no. 1, pp. 3–28, Mar. 2015.

[23] S. Pan, X. Zhao, and Y.-C. Liang, "Robust power allocation for OFDM-based cognitive radio networks: A switched affine based control approach," *IEEE Access*, vol. 5, pp. 18778–18792, 2017.

[24] G. Matsui, T. Tachibana, Y. Nakamura, and K. Sugimoto, "Distributed power adjustment based on control theory for cognitive radio networks," *Comput. Netw.*, vol. 57, no. 17, pp. 3344–3356, 2013.

[25] A. M. Mayers, P. J. Benavidez, G. V. S. Raju, D. Akopian, and M. M. Jamshidi, "A closed-loop transmission power control system using a nonlinear approximation of power-time curve," *IEEE Syst. J.*, vol. 9, no. 3, pp. 1011–1019, Sep. 2015.

[26] M. Rasti, M. Hasan, L. B. Le, and E. Hossain, "Distributed uplink power control for multi-cell cognitive radio networks," *IEEE Trans. Commun.*, vol. 63, no. 3, pp. 628–642, Mar. 2015.

[27] S. Im, H. Jeon, and H. Lee, "Autonomous distributed power control for cognitive radio networks," in *Proc. 68th IEEE Veh. Technol. Conf.*, Calgary, BC, Canada, Sep. 2008, pp. 1–5.

[28] N. Tang, S. Mao, and S. Kompella, "Power control in full duplex underlay cognitive radio networks: A control theoretic approach," in *Proc. IEEE Military Commun. Conf. (MILCOM)*, Oct. 2014, pp. 949–954.

[29] K. Shoarinejad, J. L. Speyer, and G. J. Pottie, "A distributed scheme for integrated predictive dynamic channel and power allocation in cellular radio networks," in *Proc. IEEE Global Telecommun. Conf. (GLOBECOM)*, San Antonio, TX, USA, Nov. 2001, pp. 3623–3627.

[30] F. Gunnarsson and F. Gustafsson, "Control theory aspects of power control in UMTS," *Control Eng. Pract.*, vol. 11, no. 10, pp. 1113–1125, 2003.

[31] R. F. Stengel, *Optimal Control and Estimation*. New York, NY, USA: Dover, 1994.

[32] F. Gunnarsson, "Power control in cellular radio systems: Analysis, design and estimation," Ph.D. dissertation, Dept. Elect. Eng., Linköpings Univ., Linköping, Sweden, 1998, pp. 57–62.

[33] B.-K. Lee, Y.-H. Chen, and B.-S. Chen, "Robust H∞ power control for CDMA cellular communication systems," *IEEE Trans. Signal Process.*, vol. 54, no. 10, pp. 3947–3956, Oct. 2006.

[34] Z. Wang and W. Zhang, "Spectrum sharing with limited channel feedback," *IEEE Trans. Wireless Commun.*, vol. 12, no. 5, pp. 2524–2532, May 2013.

[35] P. Massioni and M. Verhaegen, "Distributed control for identical dynamically coupled systems: A decomposition approach," *IEEE Trans. Autom. Control*, vol. 54, no. 1, pp. 124–135, Jan. 2009.

[36] D. Liberzon, *Calculus of Variations and Optimal Control Theory: A Concise Introduction*. Princeton, NJ, USA: Princeton Univ. Press, 2011.

SHUYING ZHANG received the master's degree in communication and information system from the College of Communication Engineering, Jilin University, Changchun, China, in 2016, where she is currently pursuing the Ph.D. degree. Her research interests include cognitive radio networks, resource allocation, signal processing, modern control theory, and wireless communication.
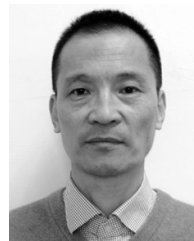
XIAOHUI ZHAO received the B.E. and M.S. degrees in electrical engineering from the Jilin University of Technology, China, in 1982 and 1989, respectively, and the Ph.D. degree in applied mathematics and control theory from the Universite de Technologie de Compiegne, France, in 1993. He was a Post-Doctoral Researcher with the Institute of Automatic Control, Southeast University, China, from 1994 to 1996. He has been a Senior Visiting Scholar with the Laboratoire d' Informatique, Universite de Pierre et Marie Curie, France, in 2006 (for half a year). He is currently a Professor of communication engineering with Jilin University. He has authored or co-authored over 100 papers of journals and international conferences, and two books in the fields of cognitive radio and signal processing. His research interests include wireless communication, cognitive radio, and adaptive signal processing. He currently serves as an Editor for the *Chinese Journal of Communications*, the *Chinese Journal of Signal Processing*, the *Chinese Journal of Internet of Things*, and the *Journal of China Universities of Posts and Telecommunications*.